Non-parabolicity and band gap re-normalisation in Si doped ZnO

R. E. Treharne* and L. J. Phillips, K. Durose

Stephenson Institute for Renewable Energy, University of Liverpool, UK

(Dated: May 22, 2013)

Abstract

PACS numbers: 78.20.Jq, 88.66.sq, 81.15.-z

Keywords: zinc oxide; magnetron sputtering; thin-film; doping; non-parabolicity, band gap normalisation

INTRODUCTION

EXPERIMENTAL METHODS

Films were deposited via RF magnetron sputtering using an AJA Phase II-J Orion system. The system was configured with a 'sputter-up' geometry with the substrate being suspended above two separate ceramic targets of ZnO and SiO_2 that were arranged off-centre and tilted at 5° towards the middle of the substrate. Soda-lime glass substrates (OptiWhite^{TM}, NSG) of size $100 \times 100 \times 4$ mm^3 were used throughout. They were cleaned by scrubbing with a nylon brush and a series of de-ionized water and isopropanol alcohol rinses followed by blow drying with a nitrogen gas jet. During deposition the ZnO and SiO_2 targets were sputtered from simultaneously using powers of 150 W and 50 W respectively. A growth pressure of 2mTorr Ar was used during deposition. The substrate temperature was maintained at 350 ± 5°C during growth and the substrate was kept static (i.e was not rotated). Deliberate gradients of both thickness and composition were subsequently achieved across the resultant film to generate a 'combinatorial' sample. A second film of pure SiO_2 was deposited under identical conditions (but without ZnO) to generate a reference film for calculating the % wt. profile of SiO_2 in the co-sputtered film.

A Shimadzu UV-Vis-IR 3700 spectrophotometer with mapping capability was used to measure the transmittance of the co-sputtered film over the range 250 - 2500 nm. 289 spectra were taken in total at 5 mm increments over the full sample surface. At each of these 289 points the sheet resistance was also measured using a CMT-SR2000 4-point probe mapping system. Following transmittance and sheet resistance measurements the sample was cut into one hundred 10×10 mm^2 pieces. A selection of these pieces, 10 in total, were further scribed into four 5×5 mm^2 sections and Hall measurement were performed on each of these sections. The Hall measurement was performed with custom built equipment, provided by Semimetrics Ltd., using a field strength of 0.8 T. Ellipsometry was performed on the same sections using a Woollam M2000-UI system. Ellipsometry was also used to map the thickness profile of the pure SiO_2 reference film.

RESULTS

Fitting of optical spectra

Figure 1 shows a typical transmittance spectra taken from a single point on the combinatorial ZnO:Si sample. The full details of the model of the dielectric permittivity, $\varepsilon(\omega)$, used to fit the data are given in [1]. The key components of the model include: 1) a Lorentzian oscillator to account for the behaviour of the system's bound electrons and to provide a smoothly varying dielectric background over the range of interest ($250 - 2500$ nm), 2) an extended Drude model [2], to characterise the system's free electron response, and 3) an inter-band transition model to account for the steep increase in the material's absorption coefficient ($\alpha \propto (E - E_G)^{1/2}$) in the vicinity of its direct band gap ($3.3 - 3.4$ eV). The two key parameters extractable from the dielectric model are the film's thickness, d, and plasma frequency, ω_p, which is related directly to the carrier concentration according to

$$\omega_p = \sqrt{\frac{n_e e^2}{m_e \varepsilon_0}} \tag{1}$$

where m_e is the effective electrons (expressed in units of the free electron mass, m_0) and ε_0 is the permittivity of free space.

Fitting was achieved by using a Nelder-Mead downhill simplex algorithm [3], implemented via python script, to minimize the quantity

$$\chi^2 = \sum_i^N \sqrt{\frac{y_i - O_i}{N^2}} \tag{2}$$

where N is the total number of data points in the spectra, O_i the observed transmittance at each wavelength over the range of interest, and y_i the theoretical transmittance calculated using the transfer matrix method [4] for a single thin-film on a finite, transparent substrate. The fitting algorithm was iterated until the relative fractional change in consecutive χ^2 values was less than 1×10^{-6}. The fitting of all 289 transmittance spectra taken over the combinatorial sample was fully automated, the only user input required being an initial estimate of film thickness at the point of the first spectrum. This automation ensured that the fitting of consecutive spectra was highly consistent. For all spectra, χ^2 values of < 1 were achieved indicating that all fits were as successful as that shown in figure 1.

It was not possible to extract accurate values for the optical band-gap E_G from the inter-band transition component of the model. All values were typically ~ 0.2 eV lower than

expected (even once non-parabolicity and re-normalisation effects had been accounted for, see sections and). This is due to the presence of a population of impurity states located in energy just below the bottom of the conduction band. The presence of these states generate a broadening, commonly referred to as an 'Urbach tail' [5], in the onset of the absorption coefficient. It is very difficult to determine the extent of this broadening by fitting the dielectric model to a single transmittance spectra. The use of variable angle spectroscopic ellipsometry (VASE) was therefore necessary to determine the true band gap of the material.

For each point over the combinatorial sample surface a set of three ellipsometric spectra, taken at angles of 60, 65 and 70° with respect to a plane normal to the sample surface, was measured and fitted using a parameterized semi-conductor (PSEMI-M0) model [6] over the range $350 - 1000$ nm. The use of multiple spectra allowed the effect of the tail states to be extricated from the direct band to band transitions. Figure 2 shows the difference in the α^2 versus E behaviour extracted from transmittance and ellipsometry data respectively. This disparity between band gaps extracted from the two techniques has been reported previously by Srikant [7].

Conduction band non-parabolicity

For highly doped metal-oxides it has been shown that the conduction band, E_c, is 'non-parabolic' and that the origin of this non-parabolicity may be attributed to a carrier dependent effective mass, $m_e(n_e)$. The functional form of this dependence, first suggested by Pisarkiewicz *et. al* [8], is given by

$$m_e(n_e) = m_{e0}\sqrt{1 + \frac{2C\hbar^2 k}{m_{e0}}} \tag{3}$$

where m_{e0} is the value of the effective mass at the conduction band minimum and C is the non-parabolicity factor, expressed in eV^{-1}. The carrier wave-number can be expressed in terms of the carrier concentration according to $k = (3\pi^2 n_e)^{1/3}$. By re-examining equation it is clear that the relationship between ω_p^2 and n_e is becomes non-linear if the effective mass is not a constant. Figure 3 shows a plot of ω_p, extracted from the spectrophotometry measurements, versus the carrier concentration, n_e^H, determined via Hall measurements, for the sample subset cut from the original combinatorial sample. A similar χ^2 minimization procedure to that described in section , in which the fitting parameters were m_{e0} and C,

was applied to the data set using

$$\chi^2 = \sum_{i=1}^{n} \frac{(n_{e_i}^S - n_{e_i}^H)^2}{n^2} \tag{4}$$

where the superscript S corresponds to carrier concentrations calculated, using a carrier dependent effecitve mass $m_e(n_e)$ (equations () a 3), from the spectroscopically determined plasma frequencies. The superscript H denotes values of n_e determined directly via Hall measurements. To determine the uncertainty associated with the fitted m_{e0} and C values a Monte-Carlo style error treatment [9] was implemented within which the $\chi 2$ minimization procedure was performed 1000 times. The inset plot in figure 3 shows the mean $m_e(n_e)$ relationship (solid line) and the corresponding spread (yellow line). An average extracted value of $m_{e0} = 0.35 \pm 0.02 m_0$ is higher than previous published values of $0.24 - 0.28 m_0$ for the effective mass in undoped ZnO. An average extracted value of $C = 0.30 \pm 0.01$ eV agrees very well with previously reported values of ~ 0.29 ev^{-1} [10, 11] for Al doped ZnO films.

CONCLUSIONS

* Corresponding Author: R.Treharne@liverpool.ac.uk

[1] R. E. Treharne, K. Hutchings, D. A. Lamb, S. J. C. Irvine, D. Lane, and K. Durose, J. Phys. D: Appl. Phys **45**, 335102 (2012).

[2] D. Mergel and Z. Qiao, J. Phys. D: Appl. Phys **35**, 794 (2002).

[3] J. A. Nelder and R. Mead, The Computer Journal **7**, 308 (1965).

[4] H. A. Macleod, *Thin-Film Optical Filters* (Adam Hilger Ltd, 1986).

[5] Urbach, .

[6] C. Herzinger, B. Johs, W. McGahan, J. Woollam, and W. Paulson, Journal of Applied Physics **83**, 3323 (1998).

[7] V. Srikant and D. R. Clarke, J. Appl. Phys. **83**, 5447 (1998).

[8] T. Pisarkiewicz and A. Kolodziej, Phys. Stat. Sol. B **158**, K5 (1990).

[9] R. J. Mendelsberg, *Photoluminescence of ZnO rown by eclipse pulsed laser deposition*, Ph.D. thesis, University of Canterbufy, New Zealand (2009).

[10] F. Ruske, A. Pflug, V. Sittinger, B. Szyszka, D. Greiner, and B. Rech, Article in press - Thin Solid Films.

[11] K. Ellmer, Journal of Physics D: Applied Physics **34**, 3097 (2001).

[12] E. Burstein, Physical Review **93**, 632 (1954).

[13] T. S. Moss, Proceedings of the Physical Society. Section B **67**, 775 (1954).

FIG. 1.

FIG. 2.

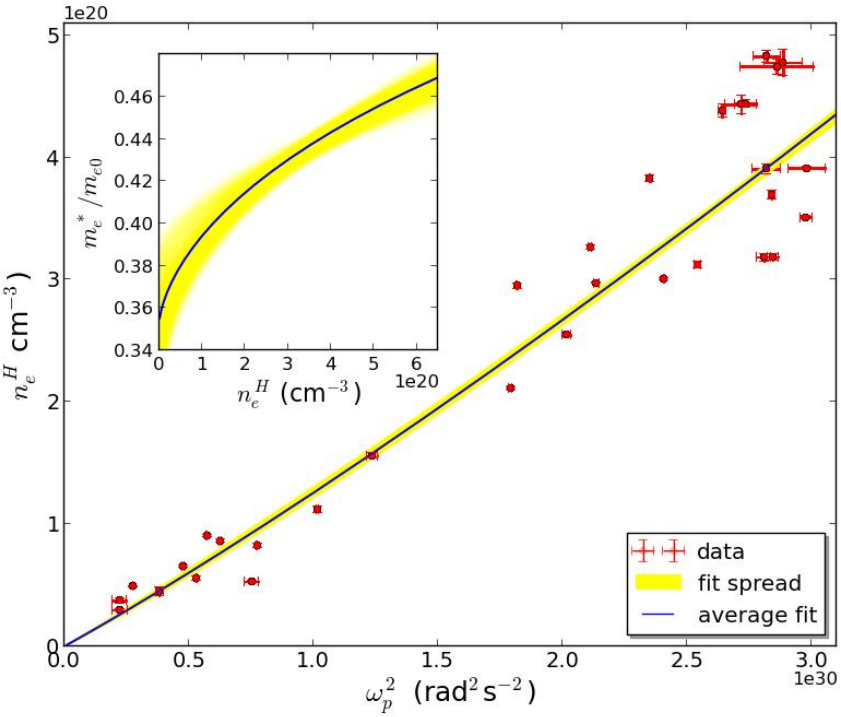

FIG. 3.

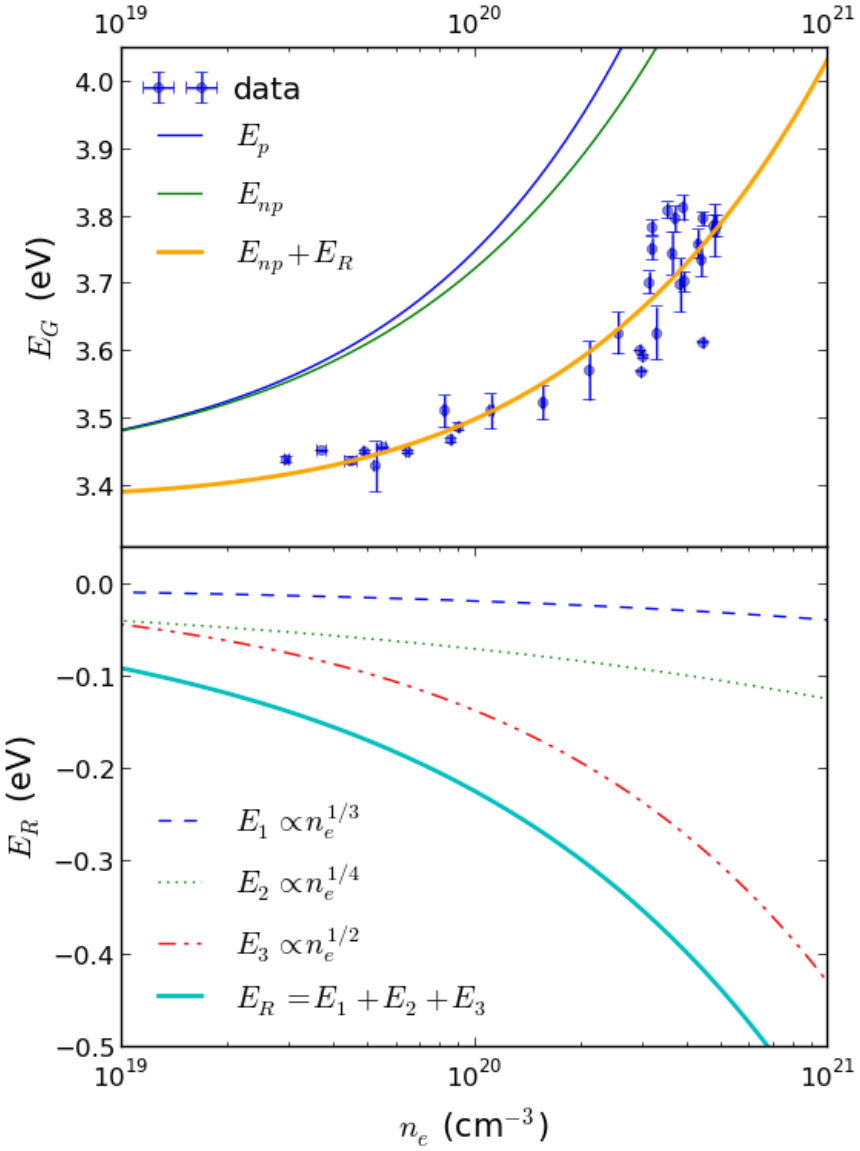
data
E_p
E_{np}
$E_{np}+E_R$
E_G (eV)
$E_1 \propto n_e^{1/3}$
$E_2 \propto n_e^{1/4}$
$E_3 \propto n_e^{1/2}$
$E_R = E_1 + E_2 + E_3$
E_R (eV)
n_e (cm^{-3})

FIG. 4.

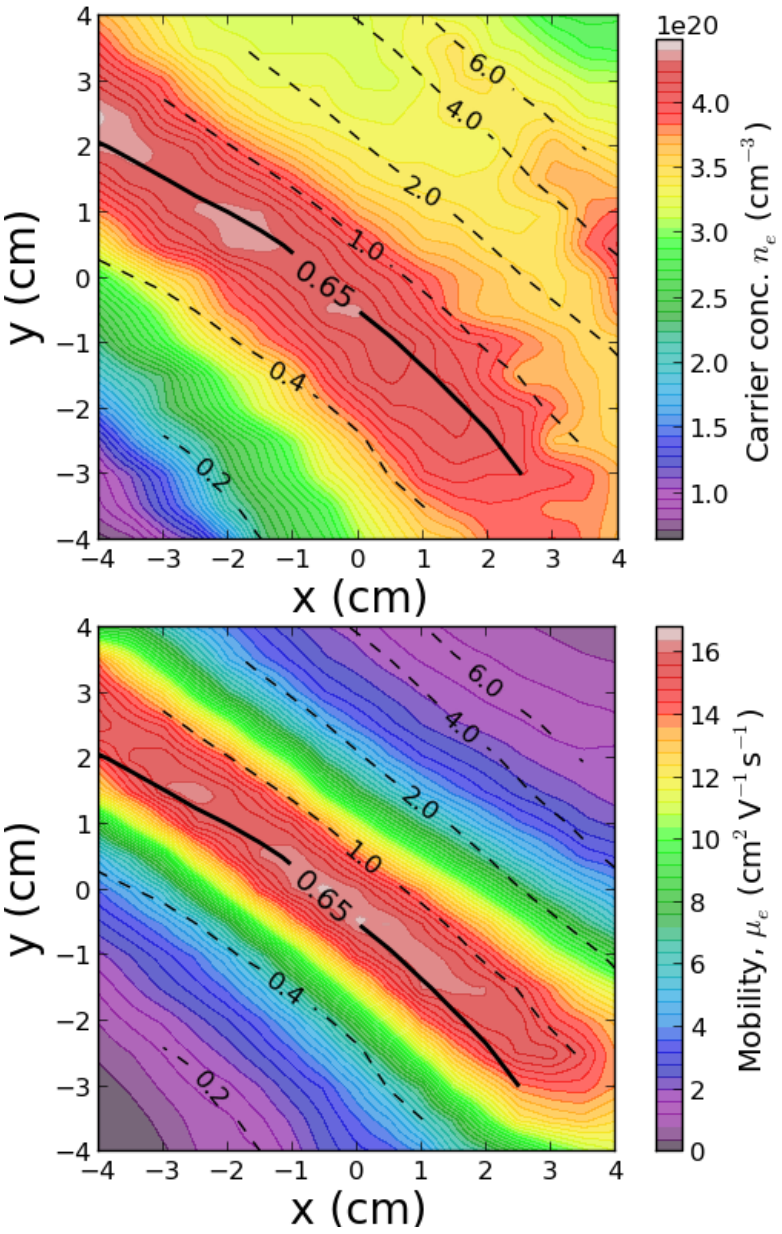

FIG. 5. Contour maps of carrier concentration and mobility over the combinatorial sample. The (–) contour lines show an overlay of the % wt. SiO_2 composition.

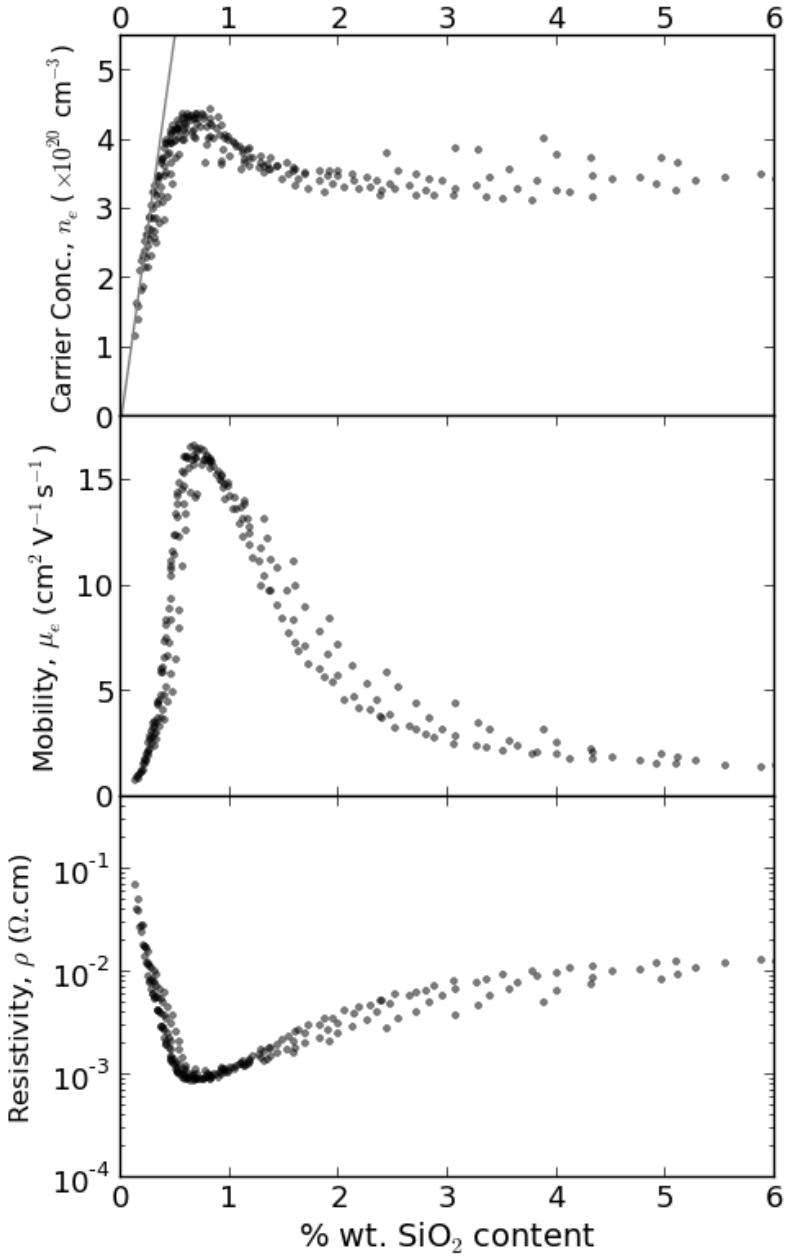

FIG. 6. Distributions of carrier concentration, mobility and resistivity with respect to % wt. SiO_2 content. The maximum values for n_e (4.4×10^{20} cm^{-3}) and μ_e (16.5 cm^{2}V^{-1}s^{-1}) coincide with a composition of 0.65% wt. SiO_2. The solid straight line in the top plot shows the maximum theoretical carrier concentration with respect to SiO_2 content should every incorporated Si atom be substituted at a Zinc site and donate 2 carriers.

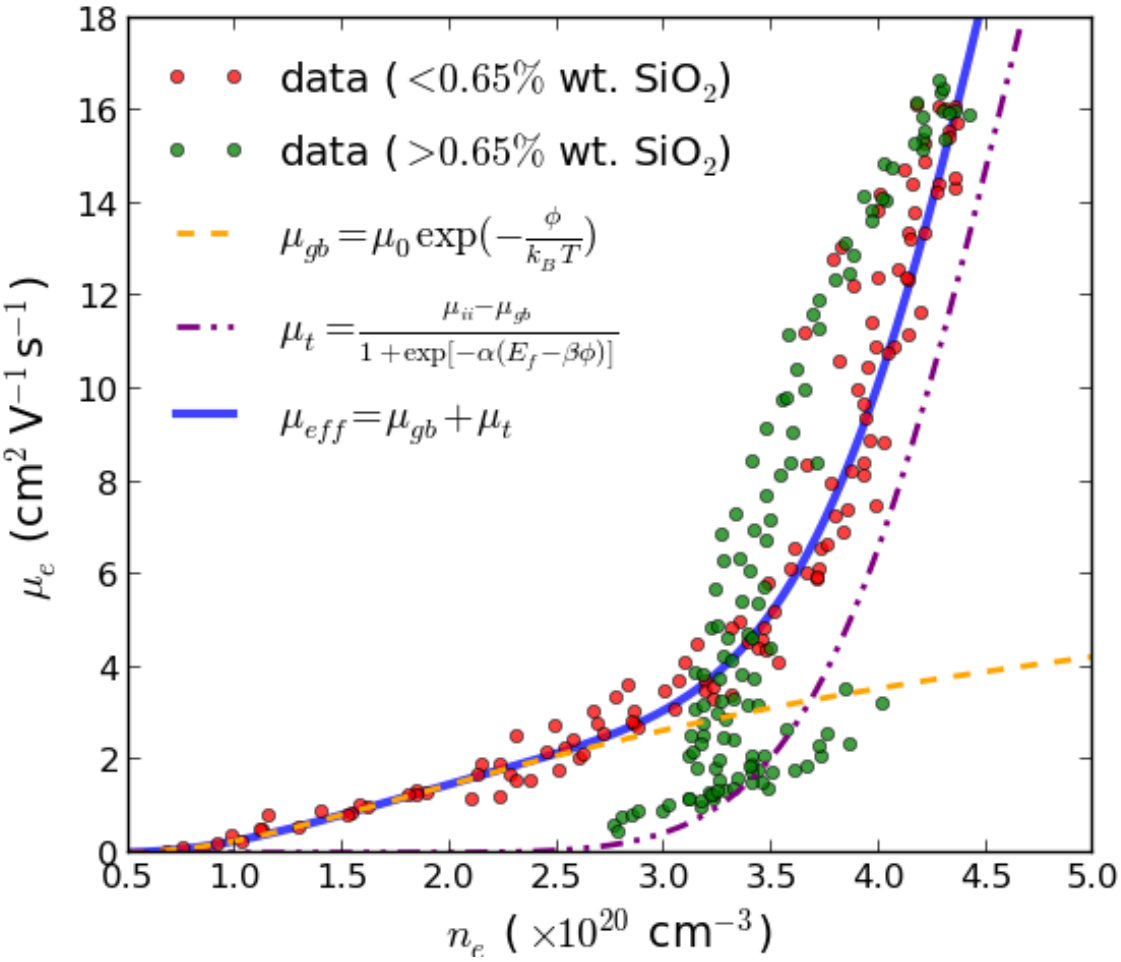
data ($<0.65\%$ wt. SiO_2)
data ($>0.65\%$ wt. SiO_2)
$\mu_{gb} = \mu_0 \exp(-\frac{\phi}{k_B T})$
$\mu_t = \frac{\mu_{ii} - \mu_{gb}}{1 + \exp[-\alpha(E_f - \beta\phi)]}$
$\mu_{eff} = \mu_{gb} + \mu_t$
μ_e ($cm^2 V^{-1} s^{-1}$)
n_e ($\times 10^{20}$ cm^{-3})
0
2
4
6
8
10
12
14
16
18
0.5
1.0
1.5
2.0
2.5
3.0
3.5
4.0
4.5
5.0

FIG. 7.